Materials Research Proceedings **22** (2022) 57-64 https://doi.org/10.21741/9781644901878-8

Exploring Electronic Structure and Optical Properties of 2D Monolayer As_2S_3 by First-Principle's Calculation

Abhishek Patel[1, a *], Deobrat Singh[2], Yogesh Sonvane[3], P.B. Thakor[1] and Rajeev Ahuja[2,4]

[1]Department of Physics, Veer Narmad South Gujarat University, Surat 395007, India

[2]Materials Theory Division, Uppsala University, Box 516, Uppsala 75120, Sweden

[3]Department of Physics, Sardar Vallabhbhai National Institute of Technology, Surat 395007, India

[4]Department of Physics, Indian Institute of Technology Ropar, Rupnagar 140001, India

* arpatel14@hotmail.com

Keywords: First-Principle's Calculation, 2D Material, Monolayer, Electronic Structure and Optical Properties

Abstract. In the present work, the structural, electronic and optical properties of the 2D monolayer As_2S_3 have been systematically investigated by the first principles calculations. The monolayer As_2S_3 has stable structure in the 2D oblique lattice which is confirm by phonon dispersion. Here, the elemental projected band-structure and density of states of the monolayer As_2S_3 have been determined by using HSE functional. The calculated bandgap of the monolayer As_2S_3 has 3.29 eV (of the indirect nature). In the optical properties, the complex dielectric function and optical absorption spectrum have been studied. The results suggest that the 2D monolayer As_2S_3 as hopeful candidate for potential applications in nano-electronics and opto-electronics.

Introduction

Among the all material families, the family of the 2D materials draw outstanding research attentions due to their remarkable electronic, mechanical, optical and others properties after the discovery and experimental realization of graphene in the year 2004[1,2]. The new members are continuously being added through theoretical predications and experimental investigations in the expanding family of 2D materials [3–6]. The 2D materials such as graphene, boron nitride (h-BN), silicene, germanene, TMDs, MXenes and etc. have high symmetric and isotropic lattice due to their hexagonal structure[7–12]. These conventional 2D materials fail to desirable performance in the direction dependent optoelectronic technology[5,13].The two-dimensional materials with low symmetry, such as borophene, phosphorene 1T' phase of TMDs and germanium phosphide have diversity in properties due to their anisotropic lattice structure[5,13]. These low symmetrical systems with diverse properties and feature can become solution for frequency and direction dependent devices due to their anisotropy[13]. The broad family of the 2D materials can fabricated by various experimental methods such as chemical vapor deposition (CVD), pulse laser deposition (PLD) method, molecular beam epitaxy (MBE) and others[14,15]. The two-dimensional (2D) semiconductor materials in the form of monolayer, bilayer and few-layers have novel combination of the electronic and optical properties[15]. It leads toward new electronic and optoelectronic devices with ultrathin thickness and flexibilities due to new physics behind their electronic structures and the screening in the 2D systems[15].

The two-dimensional (2D) materials with anisotropy can open new era of optoelectronic technology due to their orientation dependent and frequency dependent properties. The 2D black phosphorus (bP) has the large anisotropy but it is an unstable material due to its degradation in the air[13,16,17]. The 2D material with high anisotropy and stability can become a good alternative. As_2S_3 has layered structure in bulk phase and is important member of anisotropic material family. The arsenic based layered materials are useful in the electronic devices, sensors and energy system[5,18]. Recently, the 2D nanosheet of layered material As_2S_3 has been experimentally synthesized by Siskins et al.[13]. The monolayer As_2S_3 have outstanding chemical stability, high anisotropy and high thermal and dynamic stabilities[13,19]. Motivated by these interesting consequences, the structural properties, phonon-dispersion, elemental projected electronic band-structure, and optical properties of the monolayer As_2S_3 are explored using the first-principle's calculations in this work.

Computational Details

The first-principle calculations have been performed using the VASP code in this work[20,21]. The ground state energy of monolayer As_2S_3 is calculated by using the DFT calculations through Generalized Gradient Approximation (GGA) method with exchange-correlation (XC) function of Perdew-Burke-Ernzerhof (PBE)[22]. The projected augmented wave method is employed within Energy Cut-off of 500eV to approximate the core-valence electron interactions[23]. The thick vacuum of 20 Å has been inserted in the structure to avoid interaction between periodic layers in y direction[19,24–26]. By setting criteria for the total energy to 10^{-8} eV/cell and the force to 0.01 eV/Å, the structure of this material is optimized using the Monkhorst k-point grid of 7×1×7 through the conjugate gradient method[27]. Density functional perturbation theory (DPFT) calculation is performed using the supercell of the size 3×1×3 for the monolayer As_2S_3[28,29]. The phonon-dispersion of this material is calculated by using the phonopy software.[30] For the visualization of monolayer As_2S_3, the VESTA software is used[31]. To obtain accurate electronic properties of the monolayer As_2S_3, the HSE method is employed by taking screening parameter (β) = 0.2 $Å^{-1}$ and mixing parameter (α) = 0.25. The optical absorption ($\alpha(\omega)$) can be determined using the real and imaginary functions using following expressions:

$$\alpha(\omega) = \frac{4\pi E\sqrt{(|\varepsilon(\omega)|-\varepsilon_1(\omega))}}{hc}$$

where, $|\varepsilon(\omega)| = \sqrt{\varepsilon_1^2(\omega) + \varepsilon_2^2(\omega)}$, is the relative dielectric function and E is photon energy[32,33].

Results and discussion

Structural properties

The optimized structure of monolayer As_2S_3 is illustrated in the Fig.-1. In this material, the 3 coordinated As and 2 coordinated S atoms are arranged in the monoclinic lattice arrangement in Pc space group. The optimized lattice-constants of monolayer form of this 2D material are a = 4.66 Å and c =12.42 Å. While the calculated the lattice-constants of bulk-phase are a = 4.60 Å, b = 11.01 Å and c =12.26 Å. The unit-cell of monolayer As_2S_3 with two formula unit of As_2S_3 satisfies the octet rule. This monolayer material has large asymmetry due to its monoclinic arrangement in lattice space, while the other materials, like graphene, TMDs have good symmetry due to hexagonal lattice arrangement of atoms. To check the dynamic stability, the phonon band-structure for the single layer (SL) of As_2S_3 along the high symmetry path (Γ-Z-C-Y- Γ) is computed through

the DPFT method. The calculated phonon-dispersion spectra for single layer of As_2S_3 is shown in the Fig.-1(d). The positive phonon dispersion of monolayer As_2S_3 confirms the dynamic stability of structure. Here, the phonon density of states is also compatible with the phonon band-structure.

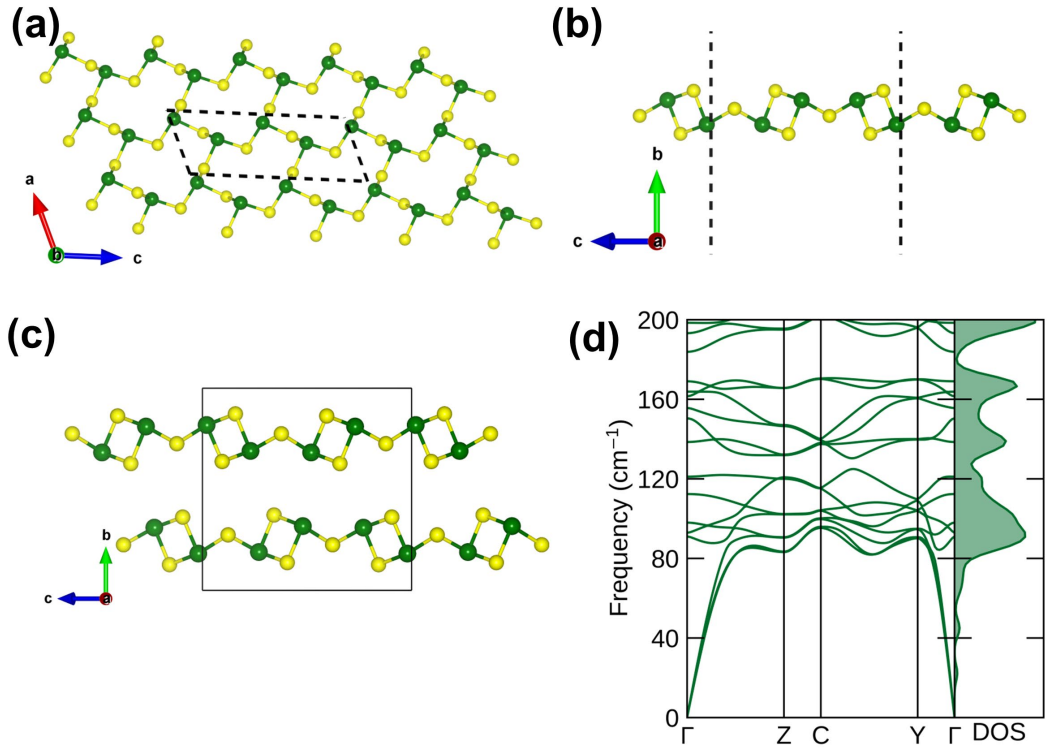

Fig.-1: (a) top view of monolayer As_2S_3, (b) sideview of monolayer As_2S_3 (c) bulk-phase of As_2S_3 and (d) phonon dispersion of monolayer As_2S_3

Electronic properties

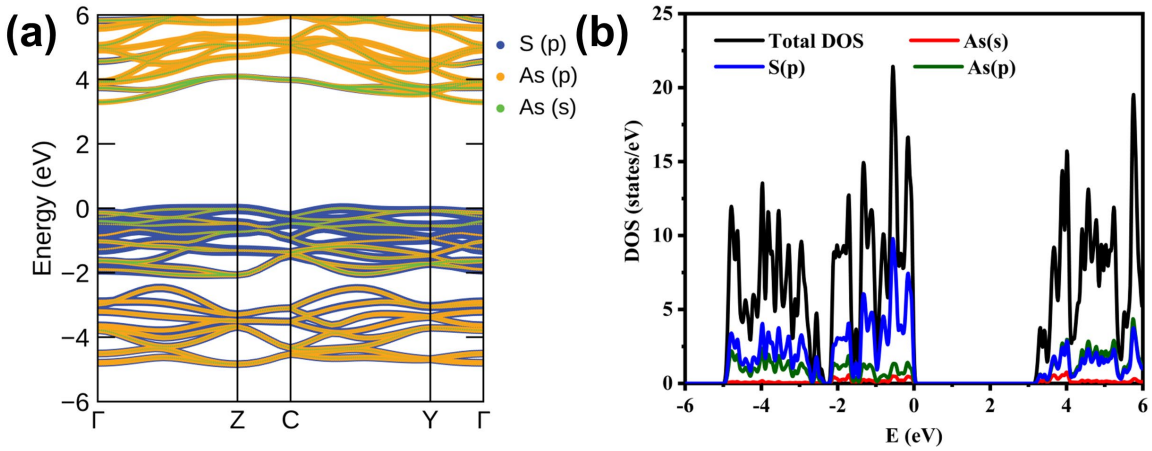

Fig.-2: (a) Electronic Band-Structure and (b) Density of States for the monolayer As_2S_3

Table 1: Electronic bandgap of 2D monolayer As_2S_3

Material	Structure	Functional	Indirect Bandgap (eV)	Direct Bandgap (eV)
As_2S_3 (monolayer)	monoclinic	HSE06	3.29	3.43
As_2S_3 (monolayer)	monoclinic	PBE	2.31	2.47

The calculated the elemental projected electronic band-structure and the projected density of states (PDOS) has been illustrated in Fig.-2. Here, the elemental projected band-structure using hybrid HSE06 is computed for the monolayer As_2S_3 along the symmetry path Γ-Z-C-X- Γ. This monolayer As_2S_3 exhibits semiconducting behavior with the indirect bandgap of 3.29 eV and the direct bandgap of 3.43 eV (see Table 1). In the elemented projected electronic band-structure of monolayer As_2S_3, it is clearly observed that the conduction band mainly composed of the contribution of p-orbital of As along with significant contribution of p-orbital of S atom and while in the composition of the valence band, the dominant contribution of p-orbital of sulfer has been observed with presence of s-orbital and p-orbital of As atom (see Fig.-2(a)). Here, the contribution of the p-orbital of As increases in valence band from near fermi-level toward far from fermi-level. From the analysis of the partial density of states of monolayer As_2S_3, the p-orbitals of arsenic (As) and sulfer(S) atoms have major contribution in the formation of total density (see Fig.-2(b)). In the conduction band, they are strongly hybridized with each other and almost equality contributes in the formation of total density. While in the valence band, the p-orbital of S atom has dominant contribution than the other orbitals. In the valence band and conduction band, there is also observed the small contribution the s-orbital of As atoms. Here, the projected density of states of the monolayer As_2S_3 is highly analogues with electronic band-structure of it.

Optical properties

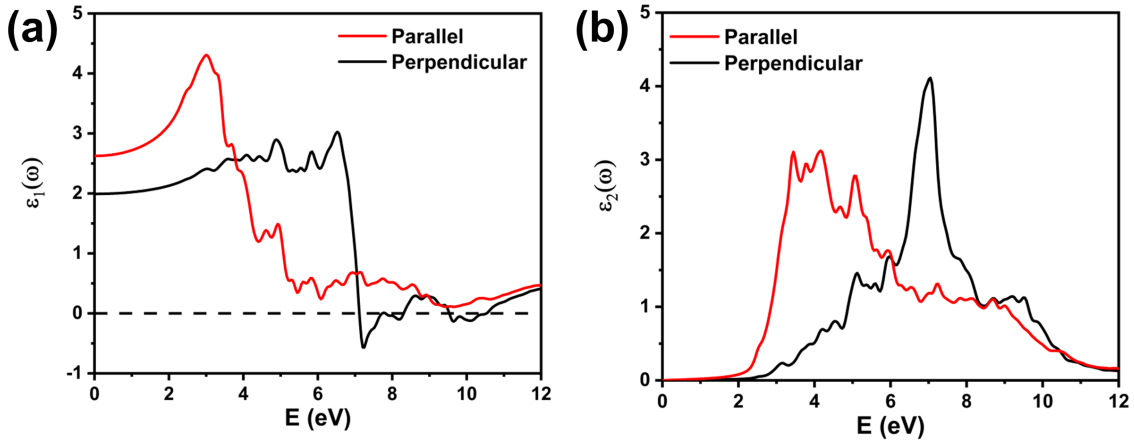

Fig.-3: Calculated complex dielectric constant of monolayer As_2S_3 :(a) real part and (b) imaginary part

The real and imaginary part of the calculated frequency dependent complex dielectric constant of 2D monolayer As_2S_3 has been illustrated in the Fig.-3. The electronic polarizability of the

material is directly related with the real dielectric function through the Clausius-Mossoti relation. The monolayer As_2S_3 shows the static value of real dielectric function (at photon energy E=0) is at 2.62 for the in-plane direction and is 1.99 for the out-plane direction (see Fig.3(a)). The maximum electronic polarizability is located at the photon energies 2.92 eV in visible region for direction parallel to field and at photon energy 7.17 eV for the perpendicular field direction. In the perpendicular field direction, the real dielectric constant shows negative values for some photon frequencies which describes metallic response for those photon energies. The monolayer As_2S_3 shows maximum negative value of real dielectric function for the photon energy 7.24 eV in UV region. While the imaginary dielectric function concerns with the electronic inter-band transitions. In direction parallel to the field, the first three peaks of imaginary dielectric constant have been located at the photon energies 3.41 eV, 3.76 eV and 4.15 eV (see Fig.3(b)). While for the case of perpendicular field direction, the first peak of imaginary dielectric constant has been observed at the photon energies 3.16 eV. The strongest peak of the imaginary dielectric function is located at photon energy 7.04 eV for the out-plane direction (perpendicular field direction).

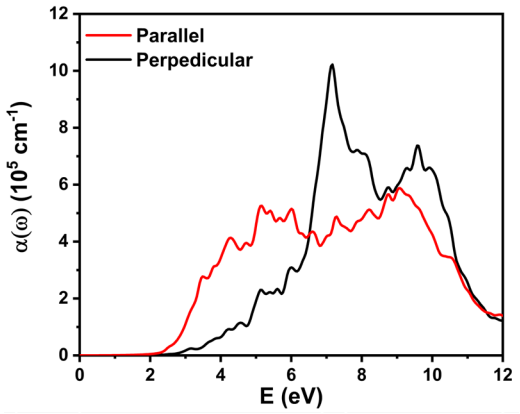

Fig.-4: Calculated optical absorption spectrum of the monolayer As_2S_3

The anisotropic optical absorption spectrum of the monolayer As_2S_3 has been illustrated in the Fig.-4. The monolayer As_2S_3 has absorption of the order 10^5 cm^{-1} for visible and UV frequencies in the both cases, parallel field and perpendicular field direction cases. For the infrared and visible frequencies having photon energy below the 2 eV, the monolayer As_2S_3 shows negligible optical absorption in both cases (in-plane direction and out-plane direction to field). In the optical absorption spectrum of monolayer As_2S_3, the large anisotropy is observed between parallel field and perpendicular field directions. This monolayer material shows the strongest absorption peak at photon energy 7.17 eV in the ultra-violet region for the out-plane direction (perpendicular direction).

Conclusion

In the present investigation, the structural, electronic properties and optical properties of 2D layered As_2S_3 have been studied for monolayer phase. The dynamically stability of monolayer phase of the 2D As_2S_3 has been confirmed by the positive phonon dispersion. The monolayer As_2S_3 is wide bandgap semiconductor with indirect electronic bandgap of 3.29 eV. This material has shown large optical absorption for visible and UV frequencies. The monolayer As_2S_3 displays anisotropic optical properties along the in-plane and out-of-plane directions. The result of the current investigation suggests the monolayer As_2S_3 for the potential applications in the field of the nanoelectronics and optoelectronics.

Conflicts of Interest
The authors declare no conflicts of interest.

Acknowledgements
A.P. is thankful to CSIR, India for his Junior Research fellowship (File No: 09/1008(0003)/2019-EMR-1). D.S. and R.A. thanks Olle Engkvists stiftelse, and Swedish Research Council (VR), Sweden for financial support. HPC2N and SNIC are acknowledged for providing the High-Performance Computing facilities.

References

[1] C. Lee, X. Wei, J.W. Kysar, J. Hone, Measurement of the Elastic Properties and Intrinsic Strength of Monolayer Graphene, Science (80-.). 321 (2008) 385 LP – 388. https://doi.org/10.1126/science.1157996

[2] D. Tyagi, H. Wang, W. Huang, L. Hu, Y. Tang, Z. Guo, Z. Ouyang, H. Zhang, Recent advances in two-dimensional-material-based sensing technology toward health and environmental monitoring applications, Nanoscale. 12 (2020) 3535–3559. https://doi.org/10.1039/C9NR10178K

[3] A.K. Geim, K.S. Novoselov, The rise of graphene, Nat. Mater. 6 (2007) 183–191. https://doi.org/10.1038/nmat1849

[4] K.S. Novoselov, A.K. Geim, S. V Morozov, D. Jiang, Y. Zhang, S. V Dubonos, I. V Grigorieva, A.A. Firsov, Electric Field Effect in Atomically Thin Carbon Films, Science (80-.). 306 (2004) 666 LP – 669. https://doi.org/10.1126/science.1102896

[5] B. Mortazavi, F. Shojaei, M. Azizi, T. Rabczuk, X. Zhuang, As2S3, As2Se3 and As2Te3 nanosheets: Superstretchable semiconductors with anisotropic carrier mobilities and optical properties, J. Mater. Chem. C. 8 (2020) 2400–2410. https://doi.org/10.1039/C9TC05904K

[6] A. Patel, D. Singh, Y. Sonvane, P.B. Thakor, R. Ahuja, Impact of stacking on the optoelectronic properties of 2D ZrS2/GaS heterostructure, Mater. Today Proc. 47 (2021) 526–528. https://doi.org/10.1016/j.matpr.2020.10.385

[7] B. Radisavljevic, A. Radenovic, J. Brivio, V. Giacometti, A. Kis, Single-layer MoS2 transistors, Nat. Nanotechnol. 6 (2011) 147–150. https://doi.org/10.1038/nnano.2010.279

[8] E. Bianco, S. Butler, S. Jiang, O.D. Restrepo, W. Windl, J.E. Goldberger, Stability and Exfoliation of Germanane: A Germanium Graphane Analogue, ACS Nano. 7 (2013) 4414–4421. https://doi.org/10.1021/nn4009406

[9] D. Nakamura, H. Nakano, Liquid-Phase Exfoliation of Germanane Based on Hansen Solubility Parameters, Chem. Mater. 30 (2018) 5333–5338. https://doi.org/10.1021/acs.chemmater.8b02153

[10] L. Song, L. Ci, H. Lu, P.B. Sorokin, C. Jin, J. Ni, A.G. Kvashnin, D.G. Kvashnin, J. Lou, B.I. Yakobson, P.M. Ajayan, Large Scale Growth and Characterization of Atomic Hexagonal Boron Nitride Layers, Nano Lett. 10 (2010) 3209–3215. https://doi.org/10.1021/nl1022139

[11] Y. Kubota, K. Watanabe, O. Tsuda, T. Taniguchi, Deep Ultraviolet Light-Emitting Hexagonal Boron Nitride Synthesized at Atmospheric Pressure, Science (80-.). 317 (2007) 932 LP – 934. https://doi.org/10.1126/science.1144216

[12] P. Vogt, P. De Padova, C. Quaresima, J. Avila, E. Frantzeskakis, M.C. Asensio, A. Resta, B. Ealet, G. Le Lay, Silicene: Compelling Experimental Evidence for Graphenelike Two-Dimensional Silicon, Phys. Rev. Lett. 108 (2012) 155501. https://doi.org/10.1103/PhysRevLett.108.155501

[13] M. Šiškins, M. Lee, F. Alijani, M.R. Van Blankenstein, D. Davidovikj, H.S.J. Van Der Zant, P.G. Steeneken, Highly Anisotropic Mechanical and Optical Properties of 2D Layered As2S3 Membranes, ACS Nano. 13 (2019) 10845–10851. https://doi.org/10.1021/acsnano.9b06161

[14] A. Zavabeti, A. Jannat, L. Zhong, A.A. Haidry, Z. Yao, J.Z. Ou, Two-Dimensional Materials in Large-Areas: Synthesis, Properties and Applications, Nano-Micro Lett. 12 (2020) 66. https://doi.org/10.1007/s40820-020-0402-x

[15] M. Bernardi, C. Ataca, M. Palummo, J.C. Grossman, Optical and Electronic Properties of Two-Dimensional Layered Materials, Nanophotonics. 6 (2017) 479–493. https://doi.org/10.1515/nanoph-2015-0030

[16] M. Moreno-Moreno, G. López-Polín, A. Castellanos-Gomez, C. Navarro, J. Gomez-Herrero, Environmental Effects in Mechanical Properties of Few-layer Black Phosphorus, 2D Mater. 3 (2016) 31007. https://doi.org/10.1088/2053-1583/3/3/031007

[17] J. Tao, W. Shen, S. Wu, L. Liu, Z. Feng, C. Wang, C. Hu, P. Yao, H. Zhang, W. Pang, X. Duan, J. Liu, C. Zhou, D. Zhang, Mechanical and Electrical Anisotropy of Few-Layer Black Phosphorus, ACS Nano. 9 (2015) 11362–11370. https://doi.org/10.1021/acsnano.5b05151

[18] S. Zhang, S. Guo, Z. Chen, Y. Wang, H. Gao, J. Gómez-Herrero, P. Ares, F. Zamora, Z. Zhu, H. Zeng, Recent progress in 2D group-VA semiconductors: from theory to experiment, Chem. Soc. Rev. 47 (2018) 982–1021. https://doi.org/10.1039/C7CS00125H

[19] A. Patel, D. Singh, Y. Sonvane, P.B. Thakor, R. Ahuja, Bulk and monolayer As2S3 as promising thermoelectric material with high conversion performance, Comput. Mater. Sci. 183 (2020) 109913. https://doi.org/10.1016/j.commatsci.2020.109913

[20] G. Kresse, J. Furthmüller, Efficient iterative schemes for ab initio total-energy calculations using a plane-wave basis set, Phys. Rev. B - Condens. Matter Mater. Phys. 54 (1996) 11169–11186. https://doi.org/10.1103/PhysRevB.54.11169

[21] G. Kresse, J. Furthmüller, Efficiency of ab-initio total energy calculations for metals and semiconductors using a plane-wave basis set, Comput. Mater. Sci. 6 (1996) 15–50. https://doi.org/10.1016/0927-0256(96)00008-0

[22] J.P. Perdew, K. Burke, M. Ernzerhof, Generalized gradient approximation made simple, Phys. Rev. Lett. 77 (1996) 3865–3868. https://doi.org/10.1103/PhysRevLett.77.3865

[23] D. Joubert, From ultrasoft pseudopotentials to the projector augmented-wave method, Phys. Rev. B - Condens. Matter Mater. Phys. 59 (1999) 1758–1775. https://doi.org/10.1103/PhysRevB.59.1758

[24] Y. Xu, Y. Li, X. Chen, C. Zhang, R. Zhang, P. Lu, First-principle study of hydrogenation on monolayer MoS2, AIP Adv. 6 (2016) 75001. https://doi.org/10.1063/1.4955430

[25] H. Li, C. Tsai, A.L. Koh, L. Cai, A.W. Contryman, A.H. Fragapane, J. Zhao, H.S. Han, H.C. Manoharan, F. Abild-Pedersen, J.K. Nørskov, X. Zheng, Activating and optimizing MoS2 basal planes for hydrogen evolution through the formation of strained sulphur vacancies, Nat. Mater. 15 (2016) 48–53. https://doi.org/10.1038/nmat4465

[26] E.N. Voronina, L.S. Novikov, Ab initio study of unzipping processes in carbon and boron nitride nanotubes under atomic oxygen impact, RSC Adv. 3 (2013) 15362–15367. https://doi.org/10.1039/c3ra41742e

[27] H.J. Monkhorst, J.D. Pack, Special points for Brillouin-zone integrations, Phys. Rev. B. 13 (1976) 5188–5192. https://doi.org/10.1103/PhysRevB.13.5188

[28] H. Shang, C. Carbogno, P. Rinke, M. Scheffler, Lattice dynamics calculations based on density-functional perturbation theory in real space, Comput. Phys. Commun. 215 (2017) 26–46. https://doi.org/10.1016/j.cpc.2017.02.001

[29] G. Kresse, J. Furthmüller, J. Hafner, Ab initio Force Constant Approach to Phonon Dispersion Relations of Diamond and Graphite, Europhys. Lett. 32 (1995) 729–734. https://doi.org/10.1209/0295-5075/32/9/005

[30] A. Togo, I. Tanaka, First principles phonon calculations in materials science, Scr. Mater. 108 (2015) 1–5. https://doi.org/10.1016/j.scriptamat.2015.07.021

[31] K. Momma, F. Izumi, VESTA 3 for three-dimensional visualization of crystal, volumetric and morphology data, J. Appl. Crystallogr. 44 (2011) 1272–1276. https://doi.org/10.1107/S0021889811038970

[32] D. Singh, S.K. Gupta, Y. Sonvane, I. Lukačević, Antimonene: a monolayer material for ultraviolet optical nanodevices, J. Mater. Chem. C. 4 (2016) 6386–6390. https://doi.org/10.1039/C6TC01913G

[33] H.R. Mahida, D. Singh, Y. Sonvane, P. Thakor, R. Ahuja, S. Gupta, The influence of edge structure on the optoelectronic properties of Si2BN quantum dot, J. Appl. Phys. 126 (2019) 0. https://doi.org/10.1063/1.5131149